

Three-loop effective potential of general scalar theory via differential equations

Bernd A. Kniehl^a, Andrey F. Pikelner^{a,b}, Oleg L. Veretin^a

^a*II. Institut für Theoretische Physik, Universität Hamburg,
Luruper Chaussee 149, 22761 Hamburg, Germany*

^b*Bogoliubov Laboratory of Theoretical Physics, Joint Institute for Nuclear Research,
141980 Dubna, Russia*

Abstract

We consider the scalar sector of a general renormalizable theory and evaluate the effective potential through three loops analytically. We encounter three-loop vacuum bubble diagrams with up to two masses and six lines, which we solve using differential equations transformed into the favorable ϵ form of dimensional regularization. The master integrals of the canonical basis thus obtained are expressed in terms of cyclotomic polylogarithms up to weight four. We also introduce an algorithm for the numerical evaluation of cyclotomic polylogarithms with multiple-precision arithmetic, which is implemented in the *Mathematica* package `cyclogpl.m` supplied here.

Keywords: Scalar theory; effective potential; cyclotomic polylogarithms

1. Introduction

The effective potential [1, 2] plays a very important role in investigating spontaneous symmetry breaking. In the Standard Model, it has been a topic of numerous studies over many years [3–7], with partial results at the three- [8] and four-loop orders [9]. The analysis of the effective potential at the two-loop order leads to the conclusion that the electroweak vacuum may be stable, critical, or slightly metastable up to very high energies of the order of the Planck scale [10–12]. Such an analysis at the three-loop order would require, apart from four-loop renormalization group functions [13–18], also the matching conditions, which are presently known through the two-loop order only [19]. An important step has recently been taken in Ref. [20], where the three-loop potential has been studied in a general renormalizable theory evaluating the loop integrals numerically [21–23].

In this work, we consider the purely scalar sector of a general renormalizable theory and evaluate the effective potential through three loops analytically. The integrals that appear in our calculation can have up to two different mass scales. In the case of $\mathcal{O}(n)$ symmetry, we reproduce the known result for the scalar φ^4 theory with spontaneous symmetry breaking. This theory is a matter of interest for the study of phase transitions, and its effective potential has been calculated in a series of papers [24, 25]. The results presented here also reproduce the contribution of the scalar sector to the effective potential in the Standard Model.

This paper is organized as follows. In Section 2, we introduce the Lagrangian of the scalar sector and parametrize the three-loop effective potential in terms of three-loop master integrals. In Section 3, we discuss the evaluation of the master integrals with two different mass scales with the help of differential equations.

In Section , we present our results. The numerical evaluation of the cyclotomic polylogarithms that appear in our results is discussed in the appendix.

2. Effective potential in the scalar theory

Let us consider the scalar theory described by the Lagrangian

$$\mathcal{L}_S = \frac{1}{2}(\partial H)^2 + \frac{1}{2}(\partial G)^2 - \frac{\mu_0^2}{2}H^2 - \frac{\mu_i^2}{2}G_i^2 - \frac{\tau_0}{6}H^3 - \frac{\tau_i}{6}HG_i^2 - \frac{\lambda_0}{24}H^4 - \frac{\lambda_i}{12}H^2G_i^2 - \frac{\lambda_{ij}}{24}G_i^2G_j^2, \quad (1)$$

where τ_i , λ_i , and λ_{ij} are couplings. In the Standard Model, the scalar part of the potential reads

$$\mathcal{L} = -m^2\Phi^\dagger\Phi - \lambda(\Phi^\dagger\Phi)^2. \quad (2)$$

In the broken phase, it can be parametrized as

$$\Phi = \frac{1}{\sqrt{2}} \begin{pmatrix} \phi + H + iG_0 \\ G^+ \end{pmatrix}, \quad (3)$$

where ϕ is the vacuum expectation value, H is the Higgs field, and G_0 and G^\pm are the scalar would-be Goldstone bosons. This parametrization corresponds to the following choice of parameters in Eq. (1):

$$\tau_0 = \tau_i = 6\lambda\phi, \quad \lambda_0 = \lambda_i = \lambda_{ij} = 6\lambda, \quad \mu_0^2 = m^2 + 3\lambda\phi^2, \quad \mu_i^2 = m^2 + \lambda\phi^2. \quad (4)$$

The three-loop contribution to the effective potential of the theory in Eq. (1) can be schematically represented as the following sum of Feynman diagrams:

$$\begin{aligned}
V_3 = & \frac{\lambda_0^2}{16} \text{ (three circles)} + \frac{2}{3} \frac{\lambda_0 \lambda_i}{16} \text{ (two circles, one dashed blue)} + \frac{1}{9} \frac{\lambda_i^2}{16} \text{ (one circle, one dashed blue)} \\
& + \frac{1}{9} \frac{\lambda_i \lambda_j}{16} \text{ (two dashed blue circles)} + \frac{2(1+2\delta_{ij})}{9} \frac{\lambda_i \lambda_{ij}}{16} \text{ (one circle, one dashed blue)} + \frac{(1+2\delta_{ij})(1+2\delta_{jk})}{9} \frac{\lambda_{ij} \lambda_{jk}}{16} \text{ (three dashed blue circles)} \quad (5)
\end{aligned}$$

$$\begin{aligned}
& + \frac{\lambda_0 \tau_0^2}{8} \text{ (two circles joined at a point)} + \frac{1}{3} \frac{\lambda_i \tau_0^2}{8} \text{ (circle with dashed blue boundary and red } i \text{)} + \frac{2}{27} \frac{\lambda_i \tau_i^2}{8} \text{ (circle with dashed blue boundary and red } i \text{)} \\
& + \frac{2(1+2\delta_{ij})}{27} \frac{\lambda_{ij} \tau_j^2}{8} \text{ (circle with dashed blue boundary and red } i, j \text{)} + \frac{1}{9} \frac{\lambda_0 \tau_i^2}{8} \text{ (two circles joined at a point)} + \frac{1}{27} \frac{\lambda_i \tau_j^2}{8} \text{ (circle with dashed blue boundary and red } i, j \text{)}
\end{aligned} \tag{6}$$

$$+ \frac{\lambda_0^2}{48} \text{ (sphere with two horizontal lines)} + \frac{2}{3} \frac{\lambda_i^2}{48} \text{ (sphere with dashed ellipse } i \text{)} + \frac{1+2\delta_{ij}}{3} \frac{\lambda_{ij}^2}{48} \text{ (sphere with dashed ellipse } ij \text{)} \quad (7)$$

$$\begin{aligned}
& + \frac{\lambda_0 \tau_0^2}{8} \text{ (circle with inscribed triangle)} + \frac{2}{9} \frac{\tau_0 \tau_i \lambda_i}{8} \text{ (circle with inscribed triangle, one dashed edge)} \\
& + \frac{4}{27} \frac{\lambda_i \tau_i^2}{8} \text{ (circle with inscribed triangle, two dashed edges)} + \frac{1+2\delta_{ij}}{27} \frac{\lambda_{ij} \tau_i \tau_j}{8} \text{ (circle with inscribed triangle, three dashed edges)}
\end{aligned} \tag{8}$$

$$+ \frac{\tau_0^4}{16} \text{ (circle with two horizontal solid lines)} + \frac{2}{9} \frac{\tau_0^2 \tau_i^2}{16} \text{ (circle with two horizontal dashed lines, top labeled } i \text{)} + \frac{4}{81} \frac{\tau_i^4}{16} \text{ (circle with two horizontal dashed lines, both labeled } i \text{)} + \frac{1}{81} \frac{\tau_i^2 \tau_j^2}{16} \text{ (circle with two horizontal dashed lines, top labeled } i \text{, bottom labeled } j \text{)} \quad (9)$$

$$+ \frac{\tau_0^4}{24} \text{ (solid circle)} + \frac{4}{9} \frac{\tau_0 \tau_i^3}{24} \text{ (dashed circle with } i \text{)} + \frac{1}{9} \frac{\tau_i^4}{24} \text{ (dashed circle with } i \text{)} . \quad (10)$$

Here, use the following notation: in each term, the symmetry and color factors are shown explicitly and the part corresponding to the scalar loop integral with all divergences properly subtracted is depicted as a figure. We use loop functions with subtracted divergences as introduced in Ref. [20] to separate the calculation of the complicated three-loop integrals from the renormalization and the calculation of the simple lower-loop integrals.

3. Evaluation of the three-loop integrals

Let us introduce some general notations. All the three-loop integrals which appear in this calculation can be mapped, depending on the masses attached to the internal lines, on one of the three topologies **A**, **B**, or **C** shown in Fig. 1. We set $m_2 = 1$ and define the ratio $x = m_1^2/m_2^2$. After this rescaling, the respective master integrals read

$$\begin{aligned} J_{n_1 \dots n_6}^A &= \int \frac{d[k_1]d[k_2]d[k_3]}{(k_1^2 + 1)^{n_1}(k_2^2 + 1)^{n_2}(k_3^2 + 1)^{n_3}(k_{12}^2 + 1)^{n_4}(k_{23}^2 + 1)^{n_5}(k_{31}^2 + 1)^{n_6}}, \\ J_{n_1 \dots n_6}^B &= \int \frac{d[k_1]d[k_2]d[k_3]}{(k_1^2 + x)^{n_1}(k_2^2 + x)^{n_2}(k_3^2 + x)^{n_3}(k_{12}^2 + 1)^{n_4}(k_{23}^2 + 1)^{n_5}(k_{31}^2 + 1)^{n_6}}, \\ J_{n_1 \dots n_6}^C &= \int \frac{d[k_1]d[k_2]d[k_3]}{(k_1^2 + 1)^{n_1}(k_2^2 + x)^{n_2}(k_3^2 + x)^{n_3}(k_{12}^2 + x)^{n_4}(k_{23}^2 + 1)^{n_5}(k_{31}^2 + x)^{n_6}}, \end{aligned} \quad (11)$$

where $k_{ab} = k_a - k_b$ and the loop integration measure is defined as $d[k_i] = d^d k / \pi^{d/2} e^{\varepsilon \gamma_E}$, with $d = 4 - 2\varepsilon$ being the dimension of space-time and γ_E being Euler's constant.

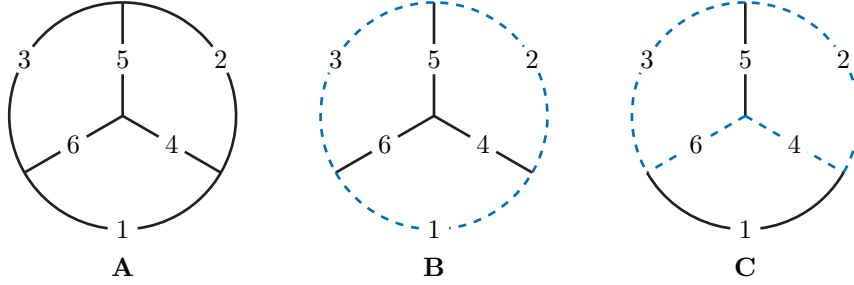


Figure 1: Topologies of the master integrals J_A , J_B , and J_C . Solid and dashed lines have mass squared $m_2^2 = 1$ and $m_1^2 = x m_2^2$, respectively.

The integrals of topology **A** are single-scale integrals and have been known for a long time [26]. Recently, they have been evaluated through weight six [27]. The integrals of topologies **B** and **C**, appearing in lines (5)–(10), have two mass scales and depend on the ratio x . For each of these two topologies, we have constructed a set of reduction rules with the help of the LiteRed package [28] and identified the set of the master integrals. Differentiating all the master integrals with respect to x and reducing the right-hand sides to the set of master integrals, we obtain the following systems of differential equations:

$$\frac{\partial J_i^b}{\partial x} = M_{ij}^b J_j^b, \quad \frac{\partial J_i^c}{\partial x} = M_{ij}^c J_j^c. \quad (12)$$

The elements of the matrices M^b and M^c are rational functions of the mass ratio x and the space-time dimension d . It is convenient to switch from the original basis $\{J^b, J^c\}$ to the new, *canonical* basis $\{g^b, g^c\}$ of master integrals introduced in Ref. [29]. The integrals in the *canonical* basis possess the property that the coefficients of their expansions in ε have uniform transcendentality weight, and the matrix of the differential equations has a special, so-called ε form.

For topologies **B** and **C**, we choose the following sets of master integrals to be transformed to the

canonical bases by suitable transformation matrices:

$$\begin{pmatrix} J_{0,0,1,0,1,1}^b \\ J_{0,1,1,0,0,1}^b \\ J_{1,1,1,0,0,0}^b \\ J_{0,0,1,1,1,1}^b \\ J_{1,1,1,0,0,1}^b \\ J_{0,1,1,0,1,1}^b \\ J_{0,1,1,1,0,1}^b \\ J_{0,1,1,1,1,1}^b \\ J_{0,2,1,1,0,1}^b \\ J_{1,1,1,0,1,1}^b \\ J_{0,1,1,1,1,1}^b \\ J_{1,1,1,1,1,1}^b \end{pmatrix} = T_b \cdot \begin{pmatrix} g_1^b \\ g_2^b \\ g_3^b \\ g_4^b \\ g_5^b \\ g_6^b \\ g_7^b \\ g_8^b \\ g_9^b \\ g_{10}^b \\ g_{11}^b \end{pmatrix}, \quad \begin{pmatrix} J_{0,0,1,0,1,1}^c \\ J_{0,0,1,1,0,1}^c \\ J_{1,0,0,0,1,1}^c \\ J_{0,0,1,1,1,1}^c \\ J_{0,1,1,1,0,1}^c \\ J_{1,0,0,1,1,1}^c \\ J_{0,1,1,1,1,1}^c \\ J_{1,0,1,1,1,0}^c \\ J_{2,0,1,1,1,0}^c \\ J_{1,0,1,1,1,1}^c \\ J_{1,1,1,1,1,1}^c \end{pmatrix} = T_c \cdot \begin{pmatrix} g_1^c \\ g_2^c \\ g_3^c \\ g_4^c \\ g_5^c \\ g_6^c \\ g_7^c \\ g_8^c \\ g_9^c \\ g_{10}^c \\ g_{11}^c \end{pmatrix}. \quad (13)$$

x

y

Figure 2: Mapping in Eq. (14).

To find the explicit forms of the transformation matrices T_b and T_c and of the matrix of the differential equations in the ε form, we use the public tools **Fuchsia** [30] and **CANONICA** [31], which are implementations of the algorithms of Refs. [32] and [33], respectively. Both algorithms heavily rely on the polynomial, rational form of the transformation matrices T_b and T_c . To fulfill this condition, we first make the variable transformation

$$x = \frac{y^2}{(1 + y^2)^2}, \quad (14)$$

illustrated in Fig. 2, upon which we can successfully find the transformation matrices T_b and T_c . The corresponding systems of differential equations then take the form

$$\frac{\partial g_i^b}{\partial y} = \varepsilon B_{ij} g_j^b, \quad \frac{\partial g_i^c}{\partial y} = \varepsilon C_{ij} g_j^c. \quad (15)$$

Now, the matrices B and C are independent of the space-time dimension d . We can proceed further and decompose them into sums of constant matrices with all dependence on the kinematic variable y factorized out. These decompositions read:

$$\begin{aligned} B(y) &= (f_0^0 B_{0,0} + f_1^0 B_{1,0} + f_2^0 B_{2,0} + f_3^0 B_{3,0} + f_3^1 B_{3,1} + f_4^1 B_{4,1} + f_6^0 B_{6,0} + f_6^1 B_{6,1} + f_{12}^1 B_{12,1} + f_{12}^3 B_{12,3}), \\ C(y) &= (f_0^0 C_{0,0} + f_1^0 C_{1,0} + f_2^0 C_{2,0} + f_3^0 C_{3,0} + f_3^1 C_{3,1} + f_4^1 C_{4,1} + f_6^0 C_{6,0} + f_6^1 C_{6,1} + f_8^3 C_{8,3}). \end{aligned} \quad (16)$$

The matrices $B_{a,b}$ and $C_{a,b}$ are constant, with rational entries, and all dependence on y is contained in the functions $f_a^b(y)$, defined as

$$f_0^0(y) = \frac{1}{y}, \quad f_a^b(y) = \frac{y^b}{\Phi_a(y)}, \quad (17)$$

where $\Phi_n(y)$ is the n -th cyclotomic polynomial relevant for our calculation. These are given by

$$\begin{aligned}
\Phi_1(y) &= y - 1, \\
\Phi_2(y) &= y + 1, \\
\Phi_3(y) &= y^2 + y + 1, \\
\Phi_4(y) &= y^2 + 1, \\
\Phi_6(y) &= y^2 - y + 1, \\
\Phi_8(y) &= y^4 + 1, \\
\Phi_{12}(y) &= y^4 - y^2 + 1.
\end{aligned} \tag{18}$$

As a nice property, these functions have transparent integration rules, which lead to a special type of functions, namely iterated integrals which generalize harmonic polylogarithms. These so-called cyclotomic harmonic polylogarithms were introduced in Ref. [34].

The systems of differential equations in ε form in Eq. (15) have the nice property that, after the expansion of all the master integrals in ε , the differential equations for the series coefficients completely decouple and can be written in the form

$$g_i^b\{\varepsilon^n\}(y) = \int_0^1 dy B_{ij} g_j^b\{\varepsilon^{n-1}\}(y) + C_{i,n}, \tag{19}$$

and similarly for topology **C**, where $g^b\{\varepsilon^n\}(y)$ denotes the $O(\varepsilon^n)$ coefficient of the ε expansion of $g^b(y)$. Integration of the decompositions in Eq. (16) leads to an iterative integration of the functions in Eq. (17). Starting from the lowest order of the expansion in ε , which is just a constant, we can integrate order by order introducing the definition of the cyclotomic harmonic polylogarithm of weight zero, $\mathcal{H}[\](y) = 1$, and using the rule

$$\mathcal{H}\left[\begin{smallmatrix} a \\ b \end{smallmatrix}; \begin{smallmatrix} a_1 \\ b_1 \end{smallmatrix}; \dots; \begin{smallmatrix} a_k \\ b_k \end{smallmatrix}\right](y) = \int dy f_a^b \mathcal{H}\left[\begin{smallmatrix} a_1 \\ b_1 \end{smallmatrix}; \dots; \begin{smallmatrix} a_k \\ b_k \end{smallmatrix}\right](y). \tag{20}$$

At each step of integration, we need to fix the integration constant. This is done by using the expansions of the integrals in the small- x limit. These expansions are not naive, but contain, on top of the power-like terms, also logarithms due to subgraphs.

4. Results

The results for the integrals in the canonical basis up to transcendental weight four can be found in the ancillary files of our submission to the arXiv. To test the validity of the obtained results, we perform a number of comparisons with already known results and carry out numerous expansions in different limits. Two-scale integrals with topologies **B** and **C** reduce in the limit $x \rightarrow e^{\frac{i\pi}{3}}$ to one-scale integrals with topology **A** and can be calculated with the help of the MATAD package. The four-line [35] and five-line [22] integrals have already been known before. Therefore, we only present here the expressions for the most complicated integrals with six lines.

After calculating all the needed integrals, we are ready to present our final results for the loop functions in lines (5)–(10). We do this for each diagram separately. Defining $L_g = \ln(m_g^2/\mu^2)$ and $L_h = \ln(m_h^2/\mu^2)$, we have for the diagrams with three one-loop subgraphs:

$$\begin{aligned}
\text{Dia[Eq. 5, 1]} &= (1 - L_h)^2 L_h m_h^4, \\
\text{Dia[Eq. 5, 2]} &= (1 - L_g)(1 - L_h) L_h m_g^2 m_h^2, \\
\text{Dia[Eq. 5, 3]} &= L_g (1 - L_h)^2 m_h^4, \\
\text{Dia[Eq. 5, 4]} &= (1 - L_g)^2 L_h m_g^4, \\
\text{Dia[Eq. 5, 5]} &= (1 - L_g) L_g (1 - L_h) m_g^2 m_h^2, \\
\text{Dia[Eq. 5, 6]} &= (1 - L_g)^2 L_g m_g^4.
\end{aligned} \tag{21}$$

For the diagrams with convolutions of two-loop and one-loop subgraphs, we have:

$$\begin{aligned}
\text{Dia}[\text{Eq. 6}, 1] &= m_h^2 \left(-\frac{3}{2}L_h^2 + \frac{1}{2}L_h^3 + \frac{3}{2}L_h(1 - 3\mathbf{S}2) - \frac{1}{2}(1 - 9\mathbf{S}2) \right), \\
\text{Dia}[\text{Eq. 6}, 2] &= m_g^2 \left((1 - L_g)L_h - \frac{1}{2}(1 - L_g)L_h^2 + \frac{1}{2}L_g(1 - 9\mathbf{S}2) - \frac{1}{2}(1 - 9\mathbf{S}2) \right), \\
\text{Dia}[\text{Eq. 6}, 3] &= \frac{(1 - L_h)m_h^2}{8(m_h^2 - 4m_g^2)} \left(m_g^2(-72 + 32L_g + 32L_h - 16L_gL_h + 32L_h^2 - 2\pi^2) \right. \\
&\quad \left. + m_h^2(-48 + 8L_g + 48L_h - 8L_gL_h + 4L_h^2 - \pi^2 - 24L_hJ_{011011}^b \{1/\varepsilon^2\} + 8J_{011011}^b \{1/\varepsilon\}) \right), \\
\text{Dia}[\text{Eq. 6}, 4] &= -\frac{(1 - L_g)m_g^2}{8(m_h^2 - 4m_g^2)} \left(m_g^2(72 - 32L_g - 32L_h + 16L_gL_h - 32L_h^2 + 2\pi^2) \right. \\
&\quad \left. + m_h^2(48 - 8L_g - 48L_h + 8L_gL_h - 4L_h^2 + \pi^2 + 24L_hJ_{011011}^b \{1/\varepsilon^2\} - 8J_{011011}^b \{1/\varepsilon\}) \right), \\
\text{Dia}[\text{Eq. 6}, 5] &= \frac{1 - L_h}{8(m_h^2 - 4m_g^2)} \left((16 - 64L_g + 8L_g^2 + 32L_h + 32L_gL_h - 24L_h^2)m_g^2m_h^2 \right. \\
&\quad \left. + m_g^4(-176 + 128L_g - 32L_g^2 + 64L_h - 32L_gL_h + 64L_h^2 - 4\pi^2) \right. \\
&\quad \left. + m_h^4(40 - 40L_h - 4L_h^2 + \pi^2) - 8m_h^2(2m_g^2 - m_h^2)(3L_hJ_{011011}^b \{1/\varepsilon^2\} - J_{011011}^b \{1/\varepsilon\}) \right), \\
\text{Dia}[\text{Eq. 6}, 6] &= -\frac{(1 - L_g)m_g^2}{8(m_h^2 - 4m_g^2)m_h^2} \left((-16 + 64L_g - 8L_g^2 - 32L_h - 32L_gL_h + 24L_h^2)m_g^2m_h^2 \right. \\
&\quad \left. + m_g^4(176 - 128L_g + 32L_g^2 - 64L_h + 32L_gL_h - 64L_h^2 + 4\pi^2) \right. \\
&\quad \left. + m_h^4(-40 + 40L_h + 4L_h^2 - \pi^2) + 8m_h^2(2m_g^2 - m_h^2)(3L_hJ_{011011}^b \{1/\varepsilon^2\} - J_{011011}^b \{1/\varepsilon\}) \right). \tag{22}
\end{aligned}$$

For the three-loop four-line diagrams, we have:

$$\begin{aligned}
\text{Dia}[\text{Eq. 7}, 1] &= \frac{m_h^4}{12} (1 + 210L_h - 132L_h^2 + 24L_h^3), \\
\text{Dia}[\text{Eq. 7}, 2] &= -8m_g^2m_h^2(2 - 8L_g + L_g^2 + 4L_h + 4L_gL_h - 3L_h^2) - m_h^4(40 - 40L_h - 4L_h^2 + \pi^2) \\
&\quad + 4m_g^4(44 - 32L_g + 8L_g^2 - 16L_h + 8L_gL_h - 16L_h^2 + \pi^2) \\
&\quad + (48L_hm_g^2m_h^2 - 24L_hm_h^4)J_{011011}^b \{1/\varepsilon^2\} + (8m_h^4 - 16m_g^2m_h^2)J_{011011}^b \{1/\varepsilon\}, \\
\text{Dia}[\text{Eq. 7}, 3] &= \frac{m_g^4}{12} (1 + 210L_g - 132L_g^2 + 24L_g^3). \tag{23}
\end{aligned}$$

For the three-loop five-line diagrams, we have:

$$\begin{aligned}
\text{Dia[Eq. 8, 1]} &= \frac{m_h^2}{3} (-97 + 78L_h - 24L_h^2 + 3L_h^3 + 162\mathbf{S2} - 81L_h\mathbf{S2} + 18\zeta_3) , \\
\text{Dia[Eq. 8, 2]} &= \frac{m_g^2}{12} (2L_g^3 - 48L_h + 24L_gL_h - 24L_h^2 - 12L_gL_h^2 + 14L_h^3 - 3\pi^2 + 3L_g\pi^2 + 8\zeta_3) \\
&\quad + \frac{m_h^2}{24} (-24 - 528L_h + 204L_h^2 + 16L_h^3 - 5\pi^2 - 6L_h\pi^2 + 648L_h\mathbf{S2} - 24\mathbf{T1ep} + 20\zeta_3) \\
&\quad + \frac{3}{2}L_h(2 + L_h)m_h^2J_{011011}^b \{1/\varepsilon^2\} - (1 + 2L_h)m_h^2J_{011011}^b \{1/\varepsilon\} + m_h^2J_{011011}^b \{\varepsilon^0\} \\
&\quad + \frac{9}{2}L_h^2m_h^2J_{011111}^b \{1/\varepsilon^2\} - 3L_hm_h^2J_{011111}^b \{1/\varepsilon\} + m_h^2J_{011111}^b \{\varepsilon^0\} , \\
\text{Dia[Eq. 8, 3]} &= \frac{m_h^2}{12} (-48L_h + 4L_h^3 - 3\pi^2 + 3L_h\pi^2 + 8\zeta_3) + \frac{m_g^2}{12} (-12 + 12L_g - 6L_g^2 + 4L_g^3 \\
&\quad - 96L_h + 48L_gL_h - 48L_h^2 - 24L_gL_h^2 + 28L_h^3 - 7\pi^2 + 6L_g\pi^2 + 16\zeta_3) \\
&\quad + 3L_h(2 + L_h)m_h^2J_{011011}^b \{1/\varepsilon^2\} - 2(1 + 2L_h)m_h^2J_{011011}^b \{1/\varepsilon\} + 2m_h^2J_{011011}^b \{\varepsilon^0\} \\
&\quad + \frac{9}{2}L_h^2m_h^2J_{111011}^b \{1/\varepsilon^2\} - 3L_hm_h^2J_{111011}^b \{1/\varepsilon\} + m_h^2J_{111011}^b \{\varepsilon^0\} , \\
\text{Dia[Eq. 8, 4]} &= \frac{m_g^2}{6} (2L_g^3 - 48L_h + 24L_gL_h - 24L_h^2 - 12L_gL_h^2 + 14L_h^3 - 3\pi^2 + 3L_g\pi^2 + 8\zeta_3) \\
&\quad + 1/12m_h^2 (-12 - 36L_h - 6L_h^2 + 4L_h^3 - 4\pi^2 + 3L_h\pi^2 + 8\zeta_3) \\
&\quad + 3L_h(2 + L_h)m_h^2J_{011011}^b \{1/\varepsilon^2\} - 2(1 + 2L_h)m_h^2J_{011011}^b \{1/\varepsilon\} + 2m_h^2J_{011011}^b \{\varepsilon^0\} \\
&\quad + 9/2L_h^2m_h^2J_{011111}^c \{1/\varepsilon^2\} - 3L_hm_h^2J_{011111}^c \{1/\varepsilon\} + m_h^2J_{011111}^c \{\varepsilon^0\} . \tag{24}
\end{aligned}$$

For the three-loop six-line diagrams of ladder type, we have:

$$\begin{aligned}
\text{Dia}[\text{Eq. 9, 1}] &= \frac{1}{3} (5 - 3L_h^2 + L_h^3 - 27(1 + L_h)\mathbf{S2} - 6\zeta_3) , \\
\text{Dia}[\text{Eq. 9, 2}] &= -\frac{1}{36m_h^2(m_h^2 - 4m_g^2)} (m_g^2m_h^2(-80 + 22L_g^3 - 24L_g^2(1 - L_h) + 17\pi^2 \\
&\quad - 3L_g(-28 + 16(5 - L_h)L_h + \pi^2 + 324\mathbf{S2}) + 2L_h(L_h(78 - 23L_h) + 3(68 - \pi^2 - 108\mathbf{S2})) \\
&\quad + 24\mathbf{T1ep} - 36\zeta_3) + m_g^4(88 - 32L_g^3 + 96L_g^2(1 - 2L_h) + 22\pi^2 - 12L_g(12 - 2L_h(34 - 7L_h) + \pi^2) \\
&\quad + 8L_h(L_h(30 + 49L_h) - 3(48 + \pi^2)) - 24\zeta_3) + m_h^4(-362 + 4L_g^3 + 12L_g^2(-3 + 2L_h) - 9\pi^2 \\
&\quad + 6L_g(28 + 8(-3 + L_h)L_h + \pi^2) - 2L_h(L_h(135 + 44L_h) - 6(56 + \pi^2 - 27\mathbf{S2})) + 486\mathbf{S2} \\
&\quad + 12\mathbf{T1ep} + 6\zeta_3) + 18L_hm_h^2((4 - 18L_h)m_g^2 + (-4 + 3L_h)m_h^2)J_{011011}^b \{1/\varepsilon^2\} \\
&\quad + 24m_h^2((-1 + 6L_h)m_g^2 + m_h^2)J_{011011}^b \{1/\varepsilon\} - 12(2m_g^2m_h^2 + m_h^4)J_{011011}^b \{\varepsilon^0\} \\
&\quad - 54L_h^2m_h^2(2m_g^2 + m_h^2)J_{011111}^b \{1/\varepsilon^2\} + 36L_hm_h^2(2m_g^2 + m_h^2)J_{011111}^b \{1/\varepsilon\} \\
&\quad - 12(2m_g^2m_h^2 + m_h^4)J_{011111}^b \{\varepsilon^0\} + 108L_h^2(m_g - m_h)m_h^2(m_g + m_h)J_{021101}^b \{1/\varepsilon^2\} \\
&\quad - 72L_hm_h^2(m_g^2 - m_h^2)J_{021101}^b \{1/\varepsilon\} + 24(m_g^2 - m_h^2)m_h^2J_{021101}^b \{\varepsilon^0\}) , \\
\text{Dia}[\text{Eq. 9, 3}] &= \frac{1}{12m_g^2(m_h^2 - 4m_g^2)} (m_g^2m_h^2(64 - 28L_g^3 - 144L_h^2 + 20L_h^3 - 6L_g^2(-7 + 4L_h) - 5\pi^2 \\
&\quad + 12L_h(-4 + \pi^2) - 3L_g(-84 + 48L_h - 12L_h^2 + \pi^2) + 8\zeta_3) - 2m_h^4(4 + 2L_g^3 - 54L_h^2 \\
&\quad - 38L_h^3 + 6L_g^2(-3 + 2L_h) - 8\pi^2 + 6L_h(10 + \pi^2) + 3L_g(28 - 24L_h + 8L_h^2 + \pi^2) + 12\zeta_3) \\
&\quad + 2m_g^4(-68 + 30L_g^3 - 48L_h^2 - 86L_h^3 + 6L_g^2(-17 + 12L_h) - 15\pi^2 + 6L_h(44 + \pi^2) \\
&\quad + 12L_g(14 - 20L_h - 2L_h^2 + \pi^2) + 20\zeta_3) + (72L_h(L_g + 3L_h)m_g^2m_h^2 - 108L_h^2m_h^4)J_{011011}^b \{1/\varepsilon^2\} \\
&\quad + (-24(L_g + 6L_h)m_g^2m_h^2 + 72L_hm_h^4)J_{011011}^b \{1/\varepsilon\} + (48m_g^2m_h^2 - 24m_h^4)J_{011011}^b \{\varepsilon^0\} \\
&\quad + (-108L_h^2m_g^2m_h^2 + 108L_h^2m_h^4)J_{021101}^b \{1/\varepsilon^2\} + (72L_hm_g^2m_h^2 - 72L_hm_h^4)J_{021101}^b \{1/\varepsilon\} \\
&\quad + (-24m_g^2m_h^2 + 24m_h^4)J_{021101}^b \{\varepsilon^0\} + (108L_h^2m_g^2m_h^2 - 54L_h^2m_h^4)J_{111011}^b \{1/\varepsilon^2\} \\
&\quad + (-72L_hm_g^2m_h^2 + 36L_hm_h^4)J_{111011}^b \{1/\varepsilon\} + (24m_g^2m_h^2 - 12m_h^4)J_{111011}^b \{\varepsilon^0\}) , \\
\text{Dia}[\text{Eq. 9, 4}] &= \frac{1}{12m_h^2(m_h^2 - 4m_g^2)} (12L_gm_g^4(44 + 8L_g^2 + 8L_g(-4 + L_h) - 16L_h(1 + L_h) + \pi^2) \\
&\quad + 4m_g^2m_h^2(4 - 6L_g^2 + L_g^3 + L_h^2(12 + 7L_h) - 3\pi^2 + 3L_g(16 - 4L_h(4 + L_h) + \pi^2) + 4\zeta_3) \\
&\quad + m_h^4(-96 - 7\pi^2 + L_h(60 + 6L_h + 4L_h^2 + 3\pi^2) + 8\zeta_3) + 24m_h^4J_{011011}^b \{\varepsilon^0\} \\
&\quad + 36L_hm_h^2(4L_gm_g^2 + L_hm_h^2)J_{011011}^b \{1/\varepsilon^2\} - 48(L_gm_g^2m_h^2 + L_hm_h^4)J_{011011}^b \{1/\varepsilon\} \\
&\quad + 54L_h^2m_h^4J_{011111}^c \{1/\varepsilon^2\} - 36L_hm_h^4J_{011111}^c \{1/\varepsilon\} + 12m_h^4J_{011111}^c \{\varepsilon^0\}) . \tag{25}
\end{aligned}$$

For the three-loop six-line diagram of Mercedes Benz type, we have:

$$\begin{aligned}
\text{Dia}[\text{Eq. 10, 1}] &= 6\zeta_3L_h - \mathbf{D6} , \\
\text{Dia}[\text{Eq. 10, 2}] &= 6\zeta_3L_h - J_{111111}^b \{\varepsilon^0\} , \\
\text{Dia}[\text{Eq. 10, 3}] &= 6\zeta_3L_h - J_{111111}^c \{\varepsilon^0\} . \tag{26}
\end{aligned}$$

The symbols $\mathbf{S2}$, $\mathbf{T1ep}$, $\mathbf{E3}$, \mathbf{DM} , \mathbf{DN} , and $\mathbf{D6}$ denote the finite and $\mathcal{O}(\varepsilon)$ parts of single-scale integrals and are defined in Ref. [26].

Here, we only present the most complicated six-line integrals:

[illegible]

[illegible]

At high energy scales, the field strength ϕ is much larger than the mass parameter m in the Lagrangian, and we can neglect the latter in Eq. (4). Thus, the ratio x is equal to $1/3$. This limit corresponds to the value $y = e^{-i\pi/6}$. For this massless version of the theory in Eq. (1), partial results are known [36, 37]. We have checked whether the expressions of all master integrals at this point can be expressed in terms of the basis constructed in Ref. [27] or a more general basis of the sixth root of unity [38]. The result is that, at weight two, this is still possible, which has already been found in Refs. [36, 37]), while, at higher weights, some other constants appear. Looking at the cyclotomic polynomials in Eq. (18), one can expect that the basis constructed from the twelfth root of unity would be appropriate.

In conclusion, we have evaluated the three-loop effective potential in the scalar sector analytically. The result is expressed in terms of cyclotomic polylogarithms of degrees 1, 2, 3, 4, 6, 8, and 12 and up to weight six. The general three-loop vacuum master integral with two different mass scales apparently does not lie in the class of polylogarithmic functions, while the particular subset relevant to the scalar sector does.

Acknowledgments

This work was supported in part by the German Federal Ministry for Education and Research BMBF through Grant No. 05H2018, by the German Research Foundation DFG through the Collaborative Research

Center No. SFB 676 *Particles, Strings and the Early Universe: the Structure of Matter and Space-Time*. The work of AFP was supported by the Foundation for the Advancement of Theoretical Physics and Mathematics “BASIS.”

Appendix A. Numerical evaluation of cyclotomic polylogarithms

In this appendix, we discuss the numerical evaluation of the cyclotomic polylogarithms. Let us consider the cyclotomic polylogarithm $\mathcal{H} \left[\begin{smallmatrix} a_w \\ b_w \end{smallmatrix}; \dots; \begin{smallmatrix} a_1 \\ b_1 \end{smallmatrix} \right] (x)$ of weight w . We introduce the following short-hand notation, omitting the argument x :

$$h_w = \mathcal{H} \left[\begin{smallmatrix} a_w \\ b_w \end{smallmatrix}; \dots; \begin{smallmatrix} a_1 \\ b_1 \end{smallmatrix} \right], \quad h_{w-1} = \mathcal{H} \left[\begin{smallmatrix} a_{w-1} \\ b_{w-1} \end{smallmatrix}; \dots; \begin{smallmatrix} a_1 \\ b_1 \end{smallmatrix} \right], \quad \dots, \quad h_1 = \mathcal{H} \left[\begin{smallmatrix} a_1 \\ b_1 \end{smallmatrix} \right], \quad h_0 = \mathcal{H} [] \equiv 1. \quad (\text{A.1})$$

Obviously, we have $(d/dx)h_k = f_{a_k}^{b_k} h_{k-1}$, $0 < k \leq w$, that is the vector of functions $\mathbf{h} = (h_w, \dots, h_0)^T$ obeys the following differential equation:

$$\frac{d}{dx} \mathbf{h} = M(x) \mathbf{h}, \quad (\text{A.2})$$

where the $(w+1) \times (w+1)$ matrix $M(x)$ has the form

$$M(x) = \begin{pmatrix} 0 & f_{a_w}^{b_w} & 0 & \dots & 0 & 0 \\ 0 & 0 & f_{a_{w-1}}^{b_{w-1}} & \dots & 0 & 0 \\ \dots & \dots & \dots & \dots & \dots & \dots \\ 0 & 0 & 0 & \dots & 0 & f_{a_1}^{b_1} \\ 0 & 0 & 0 & \dots & 0 & 0 \end{pmatrix}, \quad (\text{A.3})$$

and the rational functions $f_a^b(x)$ are given by Eq. (17). The matrix in Eq. (A.3) has simple poles at the zeros of the polynomials $\Phi_n(x)$, which are the n -th roots of unity lying on the unit circle $|x| = 1$ in the complex- x plane. There exist exactly $w+1$ linearly independent solutions \mathbf{v}_k to Eq. (A.2). It is useful to associate with this set of solutions the $(w+1) \times (w+1)$ matrix W whose columns are formed by the vectors \mathbf{v}_k . The determinant $\det W$ does not vanish at regular points of Eq. (A.3) indicating the linear independence of the solutions. Moreover, the matrix W is unique up to a constant matrix multiplier.

If, in the neighborhood of some point x_0 , the matrix $M(x)$ has a representation of the form

$$M(x) = \frac{A}{x - x_0} + \sum_{k=1}^{\infty} (x - x_0)^{k-1} M_k, \quad (\text{A.4})$$

the fundamental solution W can be found as a generalized series expansion at this point in the form (see e.g. Ref. [39])

$$W(x) = \left(\sum_{k=0}^{\infty} x^k U_k \right) x^A, \quad (\text{A.5})$$

where U_k are constant matrices given by the recursion relation

$$U_0 = I, \quad U_n A - A U_n = \sum_{k=1}^n M_k U_{n-k}. \quad (\text{A.6})$$

In particular, the solution of Eq. (A.2) around $x_0 = 0$ is given by the product

$$\mathbf{h}(x) = W(x) \mathbf{c}, \quad (\text{A.7})$$

where \mathbf{c} is the constant vector $(0, 0, \dots, 0, 1)^T$, which is determined by the boundary conditions.

In order to analytically continue $\mathbf{h}(x)$ away from $x = 0$, we follow the idea of Refs. [40, 41]. We can match the solutions in different regions at some particular point that belongs to both regions. We find that, to cover the unit circle completely, we can evaluate $W(x)$ at $x_0 = 0$ and at six other points placed symmetrically on the unit circle, $x_k = e^{i\pi k/6}$, $k = 0, 1, \dots, 5$. We fix the boundary conditions at $x_0 = 0$ as described above. The matchings to the six other expansions can be taken at the points $\tilde{x}_k = \frac{1}{2}e^{i\pi k/6}$, i.e. in the middle of the straight lines connecting x_0 and x_k .

The above algorithm has been realized in the *Mathematica* package `cyclogpl.m`. It allows one to evaluate, with multiple-precision arithmetic, the cyclotomic polylogarithms in Eq. (A.1) with $b_j \leq 12$ and arbitrary weights.

References

- [1] S. R. Coleman, E. J. Weinberg, Radiative Corrections as the Origin of Spontaneous Symmetry Breaking, *Phys. Rev. D* 7 (1973) 1888–1910. [doi:10.1103/PhysRevD.7.1888](#).
- [2] R. Jackiw, Functional evaluation of the effective potential, *Phys. Rev. D* 9 (1974) 1686. [doi:10.1103/PhysRevD.9.1686](#).
- [3] M. Sher, Electroweak Higgs Potentials and Vacuum Stability, *Phys. Rept.* 179 (1989) 273–418. [doi:10.1016/0370-1573\(89\)90061-6](#).
- [4] M. Lindner, M. Sher, H. W. Zaglauer, Probing Vacuum Stability Bounds at the Fermilab Collider, *Phys. Lett. B* 228 (1989) 139–143. [doi:10.1016/0370-2693\(89\)90540-6](#).
- [5] P. B. Arnold, S. Vokos, Instability of hot electroweak theory: bounds on $m(H)$ and $M(t)$, *Phys. Rev. D* 44 (1991) 3620–3627. [doi:10.1103/PhysRevD.44.3620](#).
- [6] C. Ford, I. Jack, D. R. T. Jones, The standard model effective potential at two loops, *Nucl. Phys. B* 387 (1992) 373–390, [Erratum: *Nucl. Phys. B* 504, 551 (1997)]. [arXiv:hep-ph/0111190](#), [doi:10.1016/0550-3213\(92\)90165-8](#), [doi:10.1016/S0550-3213\(97\)00532-4](#).
- [7] C. Ford, D. R. T. Jones, P. W. Stephenson, M. B. Einhorn, The effective potential and the renormalization group, *Nucl. Phys. B* 395 (1993) 17–34. [arXiv:hep-lat/9210033](#), [doi:10.1016/0550-3213\(93\)90206-5](#).
- [8] S. P. Martin, Three-loop Standard Model effective potential at leading order in strong and top Yukawa couplings, *Phys. Rev. D* 89 (1) (2014) 013003. [arXiv:1310.7553](#), [doi:10.1103/PhysRevD.89.013003](#).
- [9] S. P. Martin, Four-Loop Standard Model Effective Potential at Leading Order in QCD, *Phys. Rev. D* 92 (5) (2015) 054029. [arXiv:1508.00912](#), [doi:10.1103/PhysRevD.92.054029](#).
- [10] F. Bezrukov, M. Yu. Kalmykov, B. A. Kniehl, M. Shaposhnikov, Higgs Boson Mass and New Physics, *JHEP* 10 (2012) 140, [[275\(2012\)](#)]. [arXiv:1205.2893](#), [doi:10.1007/JHEP10\(2012\)140](#).
- [11] D. Buttazzo, G. Degrandi, P. P. Giardino, G. F. Giudice, F. Sala, A. Salvio, A. Strumia, Investigating the near-criticality of the Higgs boson, *JHEP* 12 (2013) 089. [arXiv:1307.3536](#), [doi:10.1007/JHEP12\(2013\)089](#).
- [12] A. V. Bednyakov, B. A. Kniehl, A. F. Pikelner, O. L. Veretin, Stability of the Electroweak Vacuum: Gauge Independence and Advanced Precision, *Phys. Rev. Lett.* 115 (20) (2015) 201802. [arXiv:1507.08833](#), [doi:10.1103/PhysRevLett.115.201802](#).
- [13] A. V. Bednyakov, A. F. Pikelner, V. N. Velizhanin, Anomalous dimensions of gauge fields and gauge coupling beta-functions in the Standard Model at three loops, *JHEP* 01 (2013) 017. [arXiv:1210.6873](#), [doi:10.1007/JHEP01\(2013\)017](#).
- [14] A. V. Bednyakov, A. F. Pikelner, V. N. Velizhanin, Yukawa coupling beta-functions in the Standard Model at three loops, *Phys. Lett. B* 722 (2013) 336–340. [arXiv:1212.6829](#), [doi:10.1016/j.physletb.2013.04.038](#).
- [15] A. V. Bednyakov, A. F. Pikelner, V. N. Velizhanin, Higgs self-coupling beta-function in the Standard Model at three loops, *Nucl. Phys. B* 875 (2013) 552–565. [arXiv:1303.4364](#), [doi:10.1016/j.nuclphysb.2013.07.015](#).
- [16] A. V. Bednyakov, A. F. Pikelner, Four-loop strong coupling beta-function in the Standard Model, *Phys. Lett. B* 762 (2016) 151–156. [arXiv:1508.02680](#), [doi:10.1016/j.physletb.2016.09.007](#).
- [17] M. F. Zoller, Top-Yukawa effects on the β -function of the strong coupling in the SM at four-loop level, *JHEP* 02 (2016) 095. [arXiv:1508.03624](#), [doi:10.1007/JHEP02\(2016\)095](#).
- [18] K. G. Chetyrkin, M. F. Zoller, Leading QCD-induced four-loop contributions to the β -function of the Higgs self-coupling in the SM and vacuum stability, *JHEP* 06 (2016) 175. [arXiv:1604.00853](#), [doi:10.1007/JHEP06\(2016\)175](#).
- [19] B. A. Kniehl, A. F. Pikelner, O. L. Veretin, Two-loop electroweak threshold corrections in the Standard Model, *Nucl. Phys. B* 896 (2015) 19–51. [arXiv:1503.02138](#), [doi:10.1016/j.nuclphysb.2015.04.010](#).
- [20] S. P. Martin, Effective potential at three loops, *Phys. Rev. D* 96 (9) (2017) 096005. [arXiv:1709.02397](#), [doi:10.1103/PhysRevD.96.096005](#).
- [21] A. Freitas, Three-loop vacuum integrals with arbitrary masses, *JHEP* 11 (2016) 145. [arXiv:1609.09159](#), [doi:10.1007/JHEP11\(2016\)145](#).
- [22] S. P. Martin, D. G. Robertson, Evaluation of the general 3-loop vacuum Feynman integral, *Phys. Rev. D* 95 (1) (2017) 016008. [arXiv:1610.07720](#), [doi:10.1103/PhysRevD.95.016008](#).
- [23] S. Bauberger, A. Freitas, TVID: Three-loop Vacuum Integrals from Dispersion relations [arXiv:1702.02996](#).
- [24] C. Ford, D. R. T. Jones, The Effective potential and the differential equations method for Feynman integrals, *Phys. Lett. B* 274 (1992) 409–414, [Erratum: *Phys. Lett. B* 285, 399 (1992)]. [doi:10.1016/0370-2693\(92\)92007-4](#).

- [25] J. M. Chung, B. K. Chung, Three loop renormalization of the effective potential, Phys. Rev. D56 (1997) 6508–6523, [Erratum: Phys. Rev.D59,109902(1999)]. [doi:10.1103/PhysRevD.59.109902](#), [doi:10.1103/PhysRevD.56.6508](#).
- [26] M. Steinhauser, MATAD: A Program package for the computation of MAssive TADpoles, Comput. Phys. Commun. 134 (2001) 335–364. [arXiv:hep-ph/0009029](#), [doi:10.1016/S0010-4655\(00\)00204-6](#).
- [27] B. A. Kniehl, A. F. Pikelner, O. L. Veretin, Three-loop massive tadpoles and polylogarithms through weight six, JHEP 08 (2017) 024. [arXiv:1705.05136](#), [doi:10.1007/JHEP08\(2017\)024](#).
- [28] R. N. Lee, Presenting LiteRed: a tool for the Loop InTEgrals REDuction [arXiv:1212.2685](#).
- [29] J. M. Henn, Multiloop integrals in dimensional regularization made simple, Phys. Rev. Lett. 110 (2013) 251601. [arXiv:1304.1806](#), [doi:10.1103/PhysRevLett.110.251601](#).
- [30] O. Gituliar, V. Magerya, Fuchsia: a tool for reducing differential equations for Feynman master integrals to epsilon form, Comput. Phys. Commun. 219 (2017) 329–338. [arXiv:1701.04269](#), [doi:10.1016/j.cpc.2017.05.004](#).
- [31] C. Meyer, Algorithmic transformation of multi-loop master integrals to a canonical basis with CANONICA, Comput. Phys. Commun. 222 (2018) 295–312. [arXiv:1705.06252](#), [doi:10.1016/j.cpc.2017.09.014](#).
- [32] R. N. Lee, Reducing differential equations for multiloop master integrals, JHEP 04 (2015) 108. [arXiv:1411.0911](#), [doi:10.1007/JHEP04\(2015\)108](#).
- [33] C. Meyer, Transforming differential equations of multi-loop Feynman integrals into canonical form, JHEP 04 (2017) 006. [arXiv:1611.01087](#), [doi:10.1007/JHEP04\(2017\)006](#).
- [34] J. Ablinger, J. Blumlein, C. Schneider, Harmonic Sums and Polylogarithms Generated by Cyclotomic Polynomials, J. Math. Phys. 52 (2011) 102301. [arXiv:1105.6063](#), [doi:10.1063/1.3629472](#).
- [35] S. Bekavac, A. G. Grozin, D. Seidel, V. A. Smirnov, Three-loop on-shell Feynman integrals with two masses, Nucl. Phys. B819 (2009) 183–200. [arXiv:0903.4760](#), [doi:10.1016/j.nuclphysb.2009.04.015](#).
- [36] J. M. Chung, B. K. Chung, Calculation of a class of three loop vacuum diagrams with two different mass values, Phys. Rev. D59 (1999) 105014. [arXiv:hep-ph/9805432](#), [doi:10.1103/PhysRevD.59.105014](#).
- [37] A. V. Kotikov, Compact analytical form for a class of three loop vacuum Feynman diagrams, JHEP 09 (1998) 001. [arXiv:hep-ph/9807440](#), [doi:10.1088/1126-6708/1998/09/001](#).
- [38] J. M. Henn, A. V. Smirnov, V. A. Smirnov, Evaluating Multiple Polylogarithm Values at Sixth Roots of Unity up to Weight Six, Nucl. Phys. B919 (2017) 315–324. [arXiv:1512.08389](#), [doi:10.1016/j.nuclphysb.2017.03.026](#).
- [39] F. Gantmakher, K. Hirsch, A. M. Society, The Theory of Matrices, no. v. 1 in AMS Chelsea Publishing Series, Chelsea Publishing Company, 2000.
- [40] R. N. Lee, A. V. Smirnov, V. A. Smirnov, Solving differential equations for Feynman integrals by expansions near singular points, JHEP 03 (2018) 008. [arXiv:1709.07525](#), [doi:10.1007/JHEP03\(2018\)008](#).
- [41] R. N. Lee, A. V. Smirnov, V. A. Smirnov, Evaluating elliptic master integrals at special kinematic values: using differential equations and their solutions via expansions near singular points, JHEP 07 (2018) 102. [arXiv:1805.00227](#), [doi:10.1007/JHEP07\(2018\)102](#).